To appear in AGU Monograph OCEAN MODELING IN AN EDDYING REGIME, Hecht and Hasumi, Eds.

Lateral Mixing in the Eddying Regime and a New Broad-Ranging Formulation

Matthew W. Hecht,[1] Elizabeth Hunke,[2] Mathew Maltrud,[2] Mark R. Petersen[1] and Beth A. Wingate[1]

Abstract. We survey a number of issues associated with lateral dissipation in eddy-resolving ocean models and present two effective techniques. The first is a specification of lateral viscosity that is closely related to that of *Chassignet and Garraffo* [2001], involving the combined application of biharmonic and Laplacian forms of viscosity. The specification can in principle be applied across a broad range of model resolution, although our testing was performed only at eddy-resolving scale where a relatively simple form suffices. The second is the implementation of the Lagrangian Averaged Navier Stokes (LANS-α) alpha subgridscale turbulence scheme in a primitive equation ocean model, with our presentation here being largely a summary of the recent work of *Hecht et al.* [2008] and *Petersen et al.* [2008]. As an inherently non-dissipative turbulence parameterization, one can understand the higher levels of eddy variability with LANS-α as coming about through an increase in the effective Rossby radius of deformation.

1. Introduction

More of the mixing processes that occur in the ocean are explicitly included in what we would refer to as eddy-resolving models, yet the parameterization of mixing remains of foremost concern. Oceanic tracer mixing may be decomposed into diabatic mixing, which tends to be very weak except under conditions of unstable stratification, and a much more vigorous adiabatic mixing. Therefore one of the great challenges of ocean modeling is the minimization of any projection of strong adiabatic mixing of tracers onto the diapycnal direction.

Whereas lateral mixing of tracers in non-eddying ocean models is nearly always formulated in an isopycnal plane, in order to mimic the way in which the unresolved eddies mix heat, salt and other tracers, it remains a matter of judgement whether to do so at the strongly eddying resolutions that we address. Along with this question, we take up the issue of more effective formulation of lateral viscosity for eddy-resolving ocean modeling. In the case of lateral viscosity, we do not distinguish between application of this strong mixing in the horizontal or isopycnal planes. We restrict our focus to the consideration of lateral mixing, both in the momentum and the tracer transport equations, as nearly all of what is known about vertical mixing has been worked out in lower resolution, non-eddy-resolving models. Vertical or diabatic mixing only enters our discussion as an unintended side effect of the specification of lateral tracer mixing.

Biharmonic forms of lateral dissipation (both viscosity and diffusivity) are most often used in simulations intended to resolve some significant level of mesoscale variability, with the simulation of the North Atlantic at 37 km scale of *Semtner and Mintz* [1977] an early example. The reason for this transition from the more physically justifiable Laplacian dissipation used at lower resolutions to the higher-order biharmonic form is a pragmatic one: The level of Laplacian dissipation required to provide adequate noise control may also strongly suppress the eddies and diffuse the jets. The reason for the limitation of hyperviscosity (or hyperdiffusivity) to the fourth-order biharmonic form in finite-difference or finite-volume ocean general circulation models is another pragmatic concern, that of maintaining a compact stencil size.

A more sophisticated usage of biharmonic lateral dissipation is the Smagorinski form of *Griffies and Hallberg* [2000], which allows for low values of viscosity in the interior while maintaining the higher values needed in the more problematic western boundary current regions, where these higher values may be needed either for numerical stability, or in order to more fully represent the viscous balance effected by eddies, if this effect is not adequately resolved.

Exceptions to the common usage of biharmonic dissipation may be found: For instance, the Ocean Circulation and Climate Advanced Modelling project (OCCAM) model uses Laplacian diffusion even at high resolution (*Lee et al.* [2002]), although this is used with a third-order upwind form of transport, for which the truncation error can be shown to be equivalent to a velocity-dependent fourth-order diffusion (*Holland et al.* [1998]). The anisotropic formulation of Laplacian viscosity introduced in *Smith and McWilliams* [2003] allows for acceptable levels of eddy activity and well-defined jets with judicious selection of parameters, including zero or nearly so, for the cross-stream component, as demonstrated in *Smith and Gent* [2004] (a paper that we bring in later for its introduction of an anisotropic form of adiabatic tracer mixing).

It is known that biharmonic dissipation can produce upgradient fluxes that are shown in *Delhez and Deleersnijder* [2007] to resemble the Gibbs phenomenon that occurs in spectral modeling. Nevertheless, biharmonic forms of dissipation continue to be used most frequently in eddy-resolving ocean modeling.

A number of simulations have used a value of biharmonic viscosity similar to that of *Smith et al.* [2000], a one-tenth degree, Mercator-grid, regional calculation in which the Gulf Stream/North Atlantic Current system compared better with observations, indicating that the variability allowed within the model, while not fully resolved in a formal sense, was sufficient to effect a considerable change in the character of the mean circulation (see *Hurlburt and Hogan* [2000], *Bryan et al.* [2007] for discussion of convergence or

[1]Computational Physics Group, CCS Division, Los Alamos National Laboratory, Los Alamos, NM, USA

[2]Fluid Dynamics Group, Theoretical Division, Los Alamos National Laboratory, Los Alamos, NM, USA

0148-0227/08/$9.00

lack thereof). *Smith et al.* scaled the coefficient of biharmonic friction with grid cell area as

$$\nu_4 = \nu_4(area_0)(area/area_0)^{3/2} \tag{1}$$

in order to maintain a constant grid Reynolds number across the grid, and hence uniform capacity to suppress noise generated by the advective operator; this point is important to later discussion (here, $\nu_4(area_0)$ refers to a reference value of biharmonic viscosity in a grid cell of area $area_0$). The lateral biharmonic tracer diffusivity was also scaled as $area^{3/2}$ in *Smith et al.* [2000].

Simulations at this one-tenth degree scale remain very sensitive, however, to the level of dissipation, as illustrated within the North Atlantic regional domain by *Bryan et al.* [2007] (hereafter BHS07). In that study the range in parameter space that produced both realistic separation of the Gulf Stream and downstream penetration of the North Atlantic Current (NAC) into the region of the Northwest Corner was seen to be very limited. These same features are also sensitive to grid discretization and boundary conditions, topics touched on in *Hecht and Smith* [2008].

In the Miami Isopycnal Coordinate Ocean Model (MICOM), *Chassignet and Garraffo* [2001] (hereafter CG01) found excessive variability in the Gulf Stream upstream from Cape Hatteras, with the Gulf Stream tending to undergo early separation, when using the same viscous prescription as *Smith et al.* [2000]; use of higher values of viscosity, on the other hand, were seen to be overly dissipative. The authors settled on a combined, isotropic approach, with biharmonic viscocity for noise control and a Laplacian form providing the viscous contribution to the balance of larger scale features. This approach has been carried over to the hybrid coordinate version of the model (HYCOM, *Bleck* [2002]). Their use of biharmonic and Laplacian viscosities together has led to our reconsideration of lateral viscosity within a simple prescription applicable across a broad range of model resolution.

We proceed to introduce this new prescription for lateral dissipation. Short review discussions of adiabatic tracer mixing (section 3) and of the implied diffusion associated with tracer advection (section 4) follow. A promising and very different approach to subgridscale turbulence parameterization, one that is inherently non-dissipative, is covered in section 5. This approach is based on the first implementation of the Lagrangian Averaged Navier Stokes alpha model (LANS-α, *Foias et al.* [2001a]) in a primitive equation ocean model, and raises the possibility of bringing out more realistic levels of oceanic mesoscale variability at what would otherwise be only eddy-admitting resolutions, thereby providing a very significant cost savings over that of conventional eddy-resolving modeling.

2. A new prescription for lateral viscosity

Our development was motivated by the success of the anisotropic form of Laplacian viscosity and by the experience of CG01 in combining isotropic forms of biharmonic and Laplacian viscocity. Sole use of biharmonic dissipation has proven more adequate in our simulations in the z-coordinate POP model (Parallel Ocean Program, *Smith and Gent* [2002]); even so, we were led to reconsider the physical and numerical roles of viscosity, and how one might articulate an overarching prescription for viscosity that would be dominated by biharmonic dissipation at high resolution and by Laplacian dissipation in the low resolution limit.

In CG01 the relative strength of biharmonic and Laplacian viscosities is presented in terms of a damping time analysis. Damping times for monochromatic waves, for Laplacian and biharmonic dissipation, are

$$\tau_2 = \nu_2^{-1}\Big(\frac{2}{\Delta x}\sin(\frac{k\Delta x}{2})\Big)^{-2}, \tag{2}$$

Table 1. Base coefficients of horizontal dissipation. Cases 14a, 14b and 14c are from BHS07, case 14x is our test case with the addition of Laplacian viscosity. Spatial scaling of coefficients is as per equation 1.

Case	ν_4	ν_2	κ_4
14a	$27.0 \times 10^9 m^4/s$	—	$9.0 \times 10^9 m^4/s$
14b	$13.5 \times 10^9 m^4/s$	—	$4.5 \times 10^9 m^4/s$
14c	$6.75 \times 10^9 m^4/s$	—	$2.25 \times 10^9 m^4/s$
14x	$6.75 \times 10^9 m^4/s$	$35.5 m^2/s$	$2.25 \times 10^9 m^4/s$

$$\tau_4 = \nu_4^{-1}\Big(\frac{2}{\Delta x}\sin(\frac{k\Delta x}{2})\Big)^{-4} \tag{3}$$

(see *Griffies* [2004]). Here, ν_2 and ν_4 are the Laplacian and biharmonic viscous coefficients, respectively, k is the wave number of the monochromatic wave that happens to be aligned, in this case, with the grid axis associated with spacing Δx. Using a small wave number approximation, as would hold for $\frac{k\Delta x}{2} \ll \frac{\pi}{2}$ and setting the two times to be equal, we solve for the wave number of the crossover point. In terms of a crossover lengthscale $\lambda_c = 2\pi/k_c$, we have

$$\lambda_c = 2\pi\sqrt{\frac{\nu_4}{\nu_2}}. \tag{4}$$

For higher wave numbers ν_4 provides the more rapid damping; for lower wave numbers ν_2 is dominant. A choice of crossover length scale of around 80 km at middle latitudes was made in CG01.

Whereas CG01 scaled both ν_4 and ν_2 for constant grid Reynolds number, resulting in the $area^{3/2}$ scaling of equation 1 and a slower $area^{1/2}$ scaling for ν_2, it suffices for one of the two terms to provide noise control and so we reconsider the scaling of the Laplacian term. We note that the level of Laplacian viscosity in CG01 was sufficient to span the width of the viscous Munk layer of the western boundary (*Munk* [1950]),

$$\delta_M = (\frac{\pi}{\sqrt{3}})(\frac{\nu_2}{\beta})^{1/3}, \tag{5}$$

with three grid lengths at the latitude of Cape Hatteras. Indeed, one would expect this to be the case, or very nearly so, as this is a second requirement of the model viscosity,

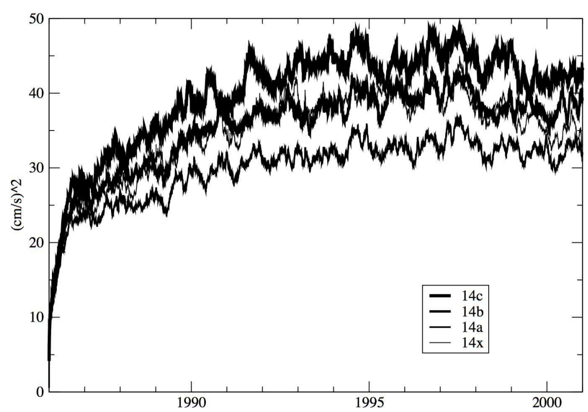

Figure 1. Mean kinetic energy, with the most viscous biharmonic case (14a) having the lowest kinetic energy, the least viscous case (14c) having the highest kinetic energy. Our test case (14x) has the the same biharmonic dissipation as case 14c, but with the addition of a Laplacian viscosity; its level of mean kinetic energy is similar to that of the intermediate case 14b. The four cases are described in Table 1.

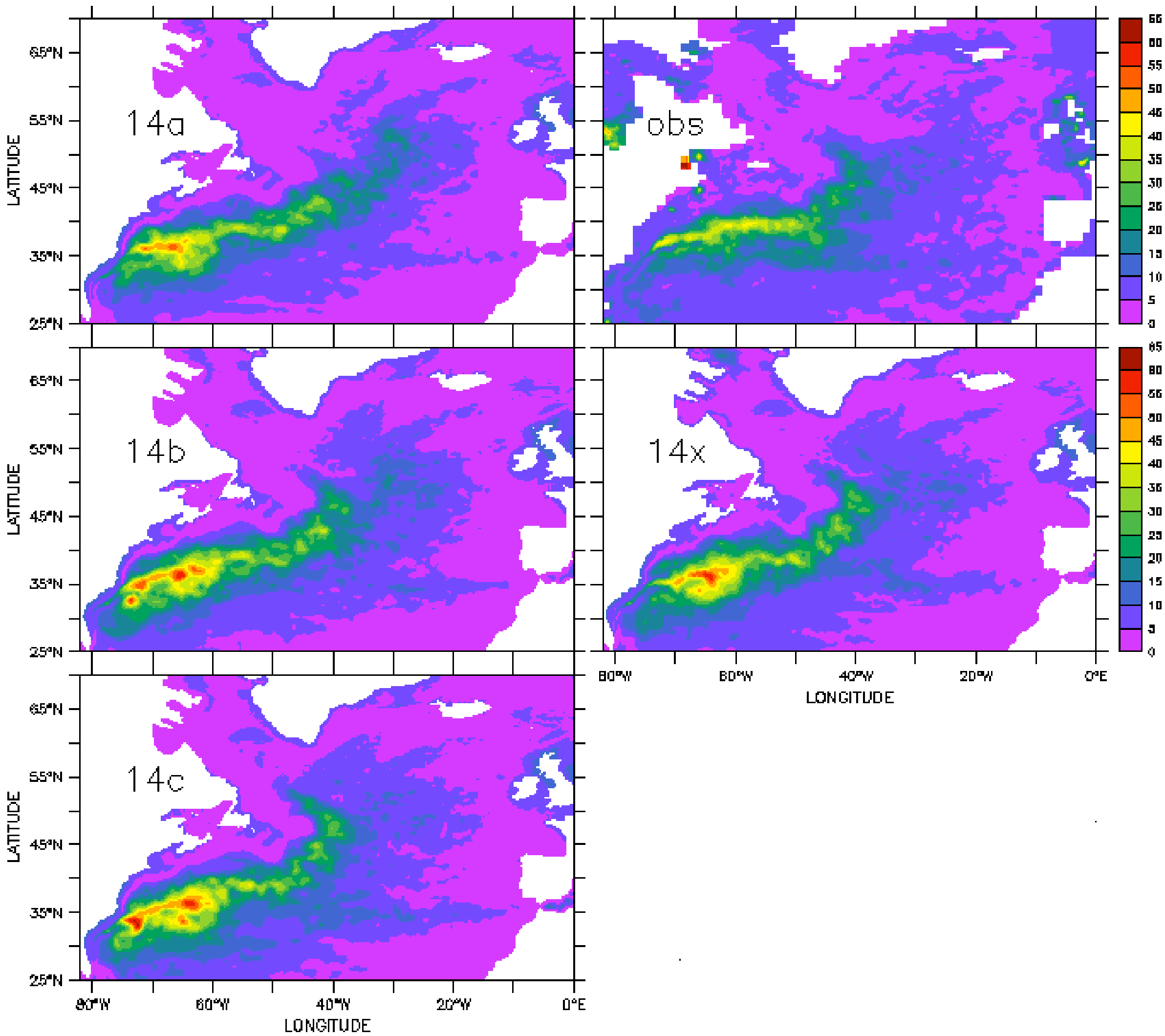

Plate 1. Time averaged North Atlantic sea surface height variability, from satellite altimetry (http://www.aviso.oceanobs.com, upper right), from the three biharmonic cases of BHS07 (left) and from our test case (lower right), all for the three year period 1998–2000. The anomalously high variability seen near the Gulf Stream's separation point in the less viscous 14b and 14c biharmonic cases is reduced in the more viscous case 14a, and in the 14x test case; the North Atlantic Current turns northward around the Grand Banks in the latter case.

more physically-based, in addition to the purely numerical requirement of noise control.

We propose a more general prescription for the use of Laplacian and biharmonic viscosity together, consisting of:

1. Laplacian viscosity scaled as Δx^3, in order to span the width of the Munk layer with a fixed number of grid lengths (of order two or three) at midlatitudes, independent of overall model resolution, and

2. biharmonic viscosity scaled as $area^{3/2}$, for noise control, as in *Smith et al.* [2000] and CG01.

If the grid is one that maintains uniform aspect ratio, with $\Delta x = \Delta y$, then the scaling of the Laplacian coefficient of prescription (1) is identical to that of the biharmonic coefficient of prescription (2), and the crossover point (where damping times for Laplacian and biharmonic terms are equal, defined in equation 4) becomes independent of grid resolution, not just within some limited mid-latitude range on a particular grid, but from the eddy-resolving regime treated in this volume to the coarse resolution (two, three or four degree) models used for long time-line paleoclimate study. In contrast, the approach of CG01 would prescribe a crossover length that grows as grid resolution in coarsened, and so is inconsistent with the widespread practice of using Laplacian viscosity at low resolution and biharmonic forms at high resolution. We adopt their combined application of biharmonic and Laplacian viscosity, but with a modified and broader-ranging spatial scaling.

We present results based on use of a crossover lengthscale (equation 4) of around $87km$ with $2\frac{1}{2}$ grid lengths across the viscous Munk layer (equation 5) at a latitude of 35°N. The coefficients used, given in Table 1, are slightly lower than those of CG01, even with our grid resolution 20% more coarse than theirs, reflecting the level of difference in explicit viscosity required in order to produce satisfactory results with two very different models (we first tried values more similar to those of CG01). If our crossover lengthscale (or that of CG01) is interpreted in terms of grid length, one sees that it falls toward the coarse end of what would be referred to as "eddy-permitting". Our prescription results in an active, primary role for the biharmonic viscosity operator in eddy-resolving applications, and in a secondary role in non-eddy-resolving application.

The values of biharmonic viscosity and diffusivity used in our test are equal to the lowest considered in BHS07; three cases from that paper, along with our test case, are listed in Table 1, where our test case is referred to as 14x. With the inclusion of Laplacian viscosity the global mean kinetic energy of case 14x is seen to drop to around the same level as that of case 14b of BHS07, where the fourth order dissipative coefficients were twice as large (see Figure 1).

The sensitivity of ocean simulations at around 1/10° is seen not only in levels of kinetic energy, but also in qualitative features, some of which would appear to be important to climate system response. The recent work of *Hallberg and Gnanadesikan* [2006] demonstrates the very different response of the Southern Ocean to changes in wind stress forcing in a simulation with a vigorous field of eddies, as compared to simulations in which the eddies are parameterized. In the North Atlantic, much attention has been paid to Gulf Stream separation, but downstream features may be more important, as discussed in this same volume by *Hecht and Smith* [2008]. *Weese and Bryan* [2006] examined North Atlantic Current bias and atmospheric circulation, attributing much of the cause of an anomalous stationary wave pattern and excessive Icelandic Low in their climate model to the sea surface temperature bias.

Not only are some of the largest sea surface temperature biases in climate simulations to be found in this southern region of the Labrador Sea, where the North Atlantic Current penetrates into the region known as the Northwest Corner (*Rossby* [1996]), but there is also the issue raised by *Hecht et al.* [2006], *Hecht and Smith* [2008]: The dense waters that convect in winter, forming a vulnerable link in the thermohaline circulation are, in ocean climate models, subject to biased conditioning as a consequence of this incorrect path.

The observed path of the North Atlantic Current is evident in satellite-based observations of altimetry, as in Plate 1 (panel at upper right). This branch of North Atlantic circulation is also produced in all the 0.1° model simulations shown except for the case with the highest values of dissipation (14a, upper left). Lower resolution simulations generally do not produce penetration of the North Atlantic Current into the Northwest Corner (again, see BHS07 and references therein). Our test case does well in this respect (lower right hand panel of Plate 1).

One of the points made in BHS07 is that deep penetration of eddy kinetic energy is correlated with reattachment of the Stream as it encounters the topography of the Southeast Newfoundland Rise (at around 48°W). The physical tendency for greater topographic control with stronger levels of eddy kinetic energy near that topography, or the converse of detachment made possible through lower levels of deep eddy kinetic energy and weaker topographic control, was cited by *Özgökmen et al.* [1997] to explain the leading-order physics upon which Gulf Stream separation depended in their somewhat idealized modeling study. This factor of greater topographic control was found, in BHS07, to be more relevant to the reattachment of the Stream at the Grand Banks than its detachment from the continental slope at Cape Hatteras. There is no obvious evidence of excessive suppression of deep eddy kinetic energy with inclusion of Laplacian viscosity in the 14x test case seen in Plate 2 at 50°W; the only one of the four cases with significantly weaker penetration of deep eddy kinetic energy is the more dissipative case 14a, the one case in which the NAC failed to make the downstream turn northward around the topography of the Grand Banks (Plate 1).

In the two less dissipative of the three cases from BHS07 there is excessive variability at the Cape Hatteras separation point, as evident in the sea surface height variability of Plate 1. The intermediate case 14b was identified as providing the best compromise between Gulf Stream separation and strong penetration of the NAC into the Northwest Corner region in BHS07. Our presciption for combined use of biharmonic and Laplacian viscosities produces an improved solution: The excess variability near Hatteras is much reduced in case 14x, even as the Gulf Stream and North Atlantic Current remain well represented. This finding of a reduction in variability at the separation point of the Gulf Stream is consistent with that of CG01.

3. Adiabatic tracer mixing

The assumption that "resolution solves all problems" is sometimes mistakenly applied to ocean modeling. Any such problem-free regime remains remote. At model resolutions of around 0.1° horizontal tracer mixing is often used, although *Roberts and Marshall* [1998] argue that spurious cross-frontal mixing should be expected to remain substantial. They consider this cross-frontal mixing (the "Veronis effect", *Veronis* [1975]) in terms of the vorticity gradient associated with the front, explaining that high levels of spurious diabatic mixing persist, even at high resolution, due to horizontal parameterization of the turbulent cascade. Model simulations at resolutions as high as 1/8° are offered in support of the authors' case.

The z-coordinate model simulations that employ adiabatic dissipation in *Roberts and Marshall* [1998] require only the thickness diffusion, or eddy-induced transport term associated with the so-called GM90 scheme of *Gent and McWilliams* [1990], because of their specification of constant salinity (if the equation of state becomes dependent only upon temperature then mixing along isopycnal surfaces reduces to zero). With only the thickness diffusion term active it is straightforward to replace the usual Laplacian form of thickness diffusion with a more scale-selective biharmonic term, preserving the eddy-resolving aspect of the 1/8° simulation. Indeed, this is an advantage held by isopycnal or hybrid z-coordinate/isopycnal models, where a complete implementation of GM90 requires only the thickness diffusion term and a biharmonic form is readily and routinely used.

A full implementation of a biharmonic form of GM90 becomes problematic in a z-coordinate model, as discussed by *Smith and Gent* [2004], who present an anisotropic Laplacian form of the scheme as an alternative to the numerically difficult biharmonic form. With this approach also motivated by the success of anisotropic forms of viscosity, they show that their solution compares favorably in terms of energetic levels, despite its Laplacian formulation. They report modest changes in the wind-driven circulation, and more substantial improvements in poleward heat transport and meridional overturning circulation, as compared with solutions based on a biharmonic form of horizontal tracer mixing. They make the interesting observation that an anisotropic tracer mixing formulation with zero cross-stream component, as was the case in their work, will not degrade an idealized front with uniform along-front values of temperature and salinity.

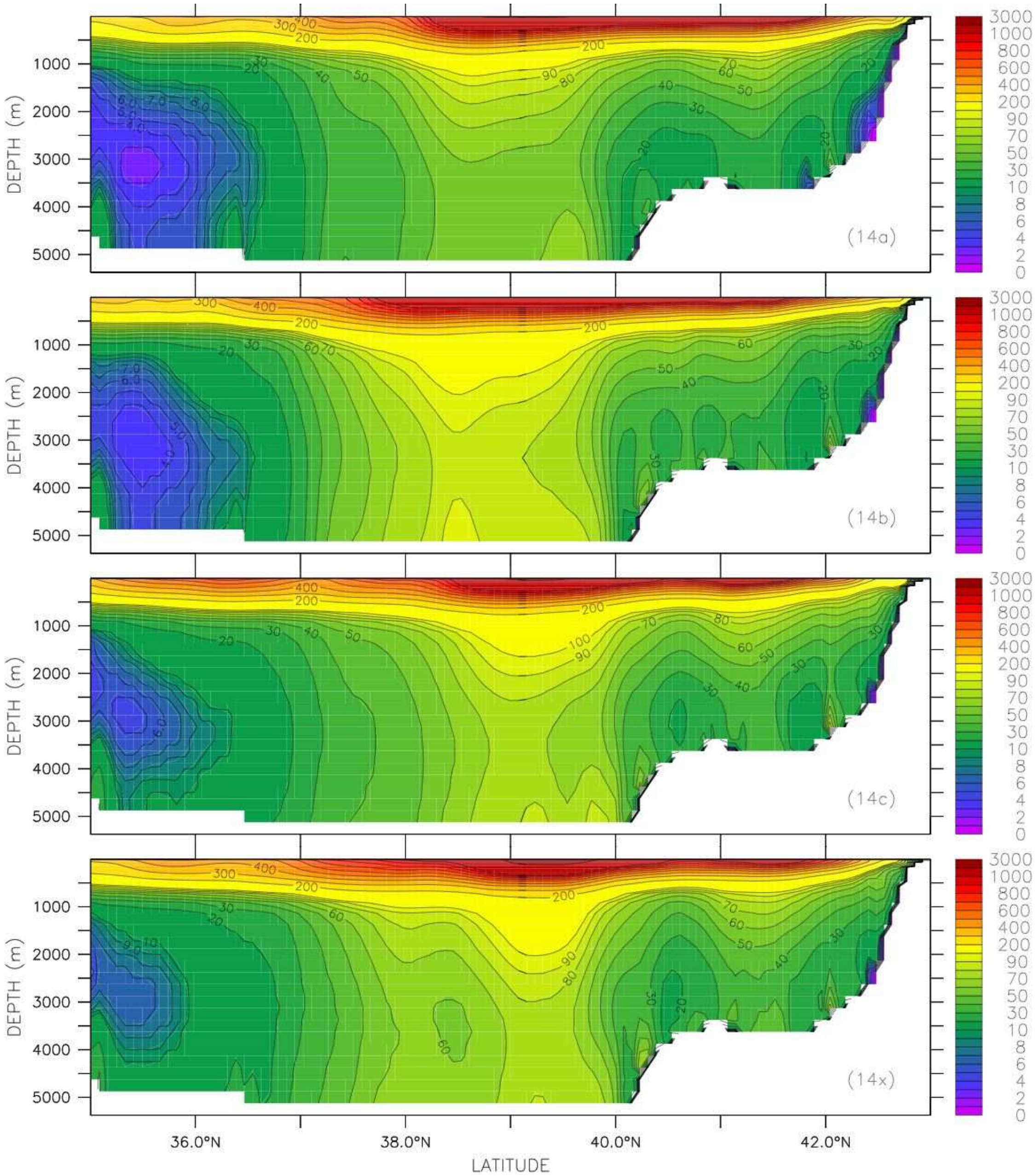

Plate 2. Eddy kinetic energies at 50°W. Our test case 14x, despite having a less energetic (and more realistic) separation of the Gulf Stream from the North American coast at Cape Hatteras (Plate 1), appears to have sufficient vertical penetration of eddy kinetic energy at this downstream point in order to successfully reattach to the continental topography at the Grand Banks. In contrast, the most viscous biharmonic case (14a) has less vertical penetration of kinetic energy and fails to make the northward turn around the Grand Banks (as was seen, again, in the earlier figure).

The work of *Smith and Gent* [2004] is not only highly relevant to the subject of this book, but deserves further investigation: It would be useful to consider anisotropic forms of viscosity and adiabatic mixing separately at 0.1° resolution, and the benefit of avoiding the Veronis effect could be evaluated more thoroughly in relation to the cost of the schemes. They also point out the need to evaluate the inherent degree of anisotropy in a strongly eddying ocean; the recent work of *Eden et al.* [2007] identifies some degree of anisotropy in eddy-driven mixing associated with Rossby wave propagation, but the extent of the effect remains to be determined.

The cost of an adiabatic tracer mixing scheme of anisotropic form is substantial, and so simple and efficient horizontal tracer mixing remains a viable choice at eddy-resolving resolution, despite the demonstrated benefit of using the more sophisticated mixing scheme. At lower, eddy-admitting resolutions, however, the cost/benefit analysis tilts in favor of adiabatic mixing.

Hunke et al. [2008] found that the anisotropic form of adiabatic tracer mixing allowed for a relatively energetic circulation in the Arctic region of their global simulation, where cells on their grid tend to be significantly smaller than in other regions. They also evaluated the use of the more conventional isotropic adiabatic tracer mixing, considering horizontal biharmonic tracer mixing, scaled as in equation 1,

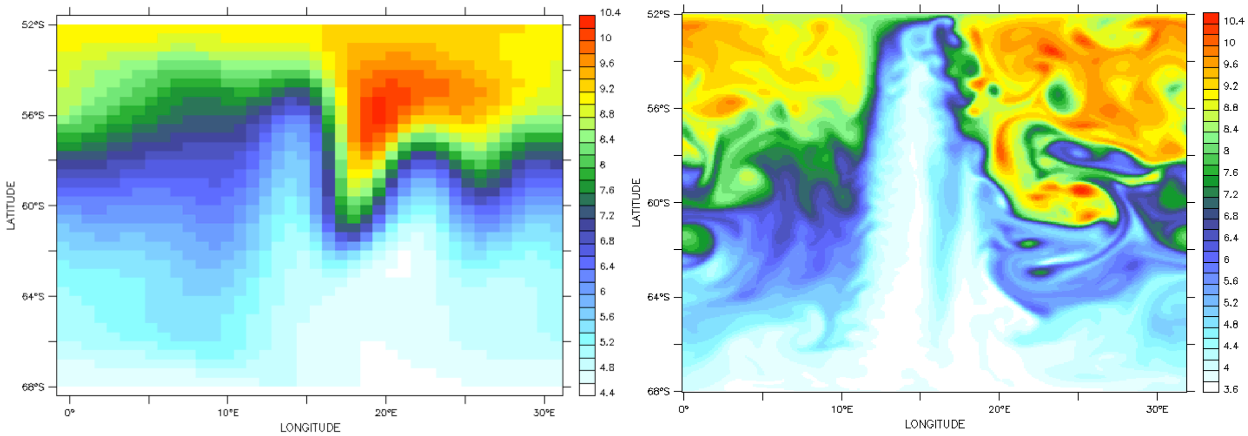

Plate 3. Sea surface temperature of the periodic channel problem used to evaluate POP-α, at low (0.8°, left) and high (0.1°, right) resolutions (but without inclusion of LANS-α here). Mesoscale eddies form if the resolution is sufficiently high.

as well. With the use of isotropic adiabatic tracer mixing they found the incorporation of spatial scaling of the mixing coefficient with grid-cell area, based on the same criteria of constant grid-Reynolds number that underlies equation 1, to be essential to bringing out an energetic model circulation in the Arctic. This scaling with grid-cell area resulted in a more modest but still significant level of improvement with the anisotropic form of the scheme.

4. Advection, truncation error and mixing

Upwind-biased advection schemes will tend to add to the overall level of mixing in a numerical ocean circulation model through a leading-order truncation error that is dissipative. Centered advection schemes, while non-dissipative, produce dispersive errors that in turn generate artificially high levels of dissipation by causing the diffusive operator, if in the tracer transport equations, to act strongly to dissipate the "ringing" associated with the dispersive error (*Hecht et al.* [1995]). The same is true in the momentum equations, where the viscous operator will tend to act to suppress dispersive errors generated by a centered discretization of momentum transport.

Griffies et al. [2000] presents a thorough testing and analysis of the truncation errors associated with the most widely used tracer transport schemes of the time, evaluating the diffusion associated with truncation error in applications as high as $1/9^\circ$ in grid resolution. They show that there are competing influences as the grid spacing is refined. The magnitude of the error tends to fall off as Δx^2. On the other hand, the lower values of explicit diffusion that one would use on a more refined grid allow for a more vigorous flow field, generating more implicit mixing from the transport scheme.

Schemes that have been adopted for use in ocean models more recently, such as that based on the work of *Hundsdorfer and Trompert* [1994] (see *Adcroft et al.* [2005], *Lindsay* [2007] for related development and application) produce significantly lower levels of implicit dissipation in these same tests (S. Griffies, personal communication). There are however some unsettling, if yet unresolved, questions associated with the use of such a scheme at eddy-resolving scale. In a revised configuration of the global model of *Maltrud and McClean* [2005], now using a tripolar grid (*Smith and Gent* [2002]) and partial cell representation of bottom topography (*Adcroft et al.* [1997]), a scheme from this newer class (in this case the tracer transport scheme of *Lindsay* [2007]) degraded the equatorial jet structure in the Pacific.

A recent line of discussion among ocean model developers concerns the question of whether adiabatic tracer mixing schemes have any physical basis at higher resolutions, or whether they are simply accomplishing the suppression of noise generated by inadequate advection schemes (again, S. Griffies, personal communication). In the near future, we will certainly see careful consideration of more advanced transport schemes in strongly eddying ocean models, in pursuit of this question. We express a note of caution, however, that the answer to this question is not yet entirely certain. The satisfactory results found by *Roberts and Marshall* [1998] and *Smith and Gent* [2004] most likely imply that dispersive errors associated with centered advection tend, in the vicinity of strong fronts, to be aligned in an along-frontal orientation. If it were not so then we would see a more significant Veronis effect in eddy-resolving models. Indeed, it should not be entirely unexpected that the spurious mixing which results from dispersive advective error should be oriented in this fashion, as the advecting velocity will also along tend to orient parallel to the front where geostrophic balance is dominant.

5. Non-Dissipative Parameterization of Turbulence for Enhanced Variability: LANS-α

In this section we give an overview of a new approach to turbulence parameterization for ocean modeling. The turbulence model itself is known as the Lagrangian Averaged Navier Stokes-α model (LANS-α, *Holm et al.* [1998]; *Holm* [1999, 2002]). This turbulence parameterization, closely related to the Generalized Lagrangian Mean theory of *Andrews and McIntyre* [1978], is derived from an averaging along mean Lagrangian trajectories (following fluid parcels) in Hamilton's Principle, yielding modified dynamical equations. The modified transport equations, which now include turbulent effects of scales smaller than α, maintain the Kelvin Circulation Theorem, meaning that the circulation around a loop embedded in the fluid neither spins up nor spins down as a result of inclusion of LANS-α. On a more pragmatic level, it means that the model is non-dissipative. Consequently, the conservation of certain quantities including total energy and potential enstrophy is maintained, making for a model with characteristics quite different from those of more familiar closures, as explained below. The model may be used in conjunction with more conventional closures, such as eddy viscosity, in order to dampen grid scale noise.

The filter width, α, can be thought of as representing the smallest active scale in the solution below which the dynamics at smaller scales is modeled as passive. These small scales are 'dragged,' or 'swept' by the fluid motion of the large scales, instead of being diffused as occurs in many other methods.

The LANS-α model has been studied extensively in the context of theory (*Holm et al.* [1998]; *Holm* [1999, 2002]; *Foias et al.* [2001b]), direct numerical simulations (*Chen et al.* [1998, 1999a, b]), fluid instability (*Holm and Wingate* [2005]), quasi-geostrophy (*Holm and Nadiga* [2003]), Large Eddy Simulations (*Domaradzki and Holm* [2001]; *Geurts and Holm* [2003]) and the shallow water equations (*Wingate* [2004]); for a review see *Holm et al.* [2005].

One feature of this model that is particularly relevant to ocean modeling was discussed by *Holm and Wingate* [2005] who showed that, for a two layer baroclinic instability problem, the alpha model had the effect of moving the Rossby deformation radius to lower wave number such that instability can occur on a coarser mesh. Essentially, one can bring energetic mesoscale variability into an ocean model at what would otherwise be only eddy-admitting resolution.

The first implementation of LANS-α in a primitive equation ocean model has been described by *Hecht et al.* [2008], with further investigation of efficiency in *Petersen et al.* [2008]. In brief, the primitive equations are modified as

$$\frac{d\mathbf{v}}{dt} + \sum_j v_j \nabla u_j + \mathbf{f} \times \mathbf{u} = -\frac{1}{\rho_0}\nabla\pi + \mathcal{F}(\mathbf{v}), \quad (6)$$

$$\frac{d\varphi}{dt} = \mathcal{D}(\varphi), \quad (7)$$

$$\frac{d}{dt} = \frac{\partial}{\partial t} + \mathbf{u}\cdot\nabla + u_3\partial_z \quad (8)$$

$$\sum_j v_j \frac{\partial u_j}{\partial z} + \frac{\partial \pi}{\partial z} = -\rho g, \quad (9)$$

$$\nabla\cdot\mathbf{u} + \partial_z u_3 = 0, \quad (10)$$

$$\mathbf{u} = \left(1 - \alpha^2\nabla^2\right)^{-1}\mathbf{v}, \quad (11)$$

$$\pi = p - \frac{1}{2}|\mathbf{u}|^2 - \frac{\alpha^2}{2}|\nabla\mathbf{u}|^2, \quad (12)$$

b where π is a modified pressure, φ is a tracer, and $\mathcal{F}$ and $\mathcal{D}$ are diffusion operators. One should note that there are now two velocities in the ocean model, a smooth velocity $\mathbf{u}$, only containing scales greater than α, that performs the transport, and a rough velocity $\mathbf{v}$ that is transported by the flow. These two velocites are related through the Helmholtz operation of equation (11).

In the case when the density is a linear function of salinity and temperature, rotation is constant, and in the absence of dissipation these equations have the following conservation laws,

$$\frac{d}{dt}\int_V (|\mathbf{u}|^2 + \alpha^2|\nabla\mathbf{u}|^2 + \rho^2) = 0 \quad (13)$$

$$\frac{d}{dt}\int_V q = 0 \quad (14)$$

where

$$q = \nabla_3\rho\cdot((\nabla_3\times\mathbf{v}_H) + f. \quad (15)$$

The LANS-α turbulence parameterization was implemented in the POP primitive equation ocean model (referred to collectively as POP-α) with the addition of the smooth advecting velocity $\mathbf{u}$. This velocity may be obtained using the Helmholtz inversion of equation (11) or by a convolution filter that simply smooths the $\mathbf{v}$ velocity by averaging over neighboring grid cells. The filter is more computationally efficient, and has been shown to produce results equivalent to those from the Helmholtz inversion (*Petersen et al.* [2008]).

The proper implementation of LANS-α in the barotropic solver of the POP model presented a particularly difficult challenge. The barotropic solver includes an iterative solution for the surface elevation, and the formal derivation of LANS-α in the POP algorithm requires smoothing steps within each iteration. That proved to be too expensive, so a reduced algorithm was designed that avoids the smoothing within the iterative step, thereby improving efficiency greatly while producing results nearly identical to those found with the full LANS-α model (*Hecht et al.* [2008]).

The POP-α algorithms and smoothing methods were tested using an idealized configuration that induces baroclinic instability. The domain is a zonally periodic channel with a meridional deep-sea ridge, westerly wind forcing, and surface thermal forcing that is warm in the north and cool in the south. These conditions are similar to those in the Southern Ocean, and cause the isopycnals to tilt downward from south to north. In the real ocean, mesoscale eddies transfer heat and flatten the isopycnals, thereby converting the potential energy of tilted isopycnals to the kinetic energy of the eddies themselves. In ocean models, this only occurs if the resolution is sufficient for eddies to appear in the simulations (Figures 3 and 2e). Thus the slope of the isopycnals is an additional diagnostic to measure eddy activity in this test problem.

LANS-α improves the representation of turbulence in all statistics measured in the channel configuration. In general, the turbulence model becomes more effective as the smoothing operator on $\mathbf{u}$ is strengthened. This can be accomplished by increasing the α parameter in the Helmholtz operator of equation (11) or by using a larger filter stencil. Figure 2 shows that both methods flatten the isopycnals and increase kinetic energy and eddy kinetic energy. The ability to increase eddy activity is a unique feature of the LANS-alpha model; other turbulence closure models, such as eddy viscosity and hyperviscosity, reduce kinetic and eddy kinetic energy. *Holm and Wingate* [2005] showed that LANS-alpha preserves the value of forcing required for the onset of baroclinic instability, while eddy viscosity models increase the required forcing so that eddies are less likely to appear.

It is possible to bring out an unrealistic level of variability with use of an overly large filter width α, as demonstrated by *Holm and Nadiga* [2003]. Tuning is required for optimal results, as with other parameterizations. We have indeed found that POP-α can produce turbulence statistics similar to a doubling of resolution or greater, and only requires an additional 27% computational time (in the most efficient implementation) as compared to a factor of eight to ten in computational time to double the horizontal resolution (*Petersen et al.* [2008]).

6. Summary discussion

We have presented in section 2 a simple method of combining Laplacian and biharmonic forms of viscosity, and have found this prescription to be effective in reducing the excessive variability near the Gulf Stream's separation point of Cape Hatteras, consistent with the experience of CG01. Our prescription is designed for use over a broad range of resolutions, with biharmonic viscosity providing noise control and Laplacian viscosity providing viscous balance over the western boundary current regions. This method has been demonstrated in the context of viscous dissipation in an eddy-resolving regional simulation of the North Atlantic Ocean. The basic scheme can be extended readily to more sophisticated anisotropic schemes, where our prescription for the scaling of the coefficient of Laplacian viscosity with grid resolution would provide the cross-stream or zonal component in the western boundary regions. Use in non-eddy-resolving models will most likely require such an extension.

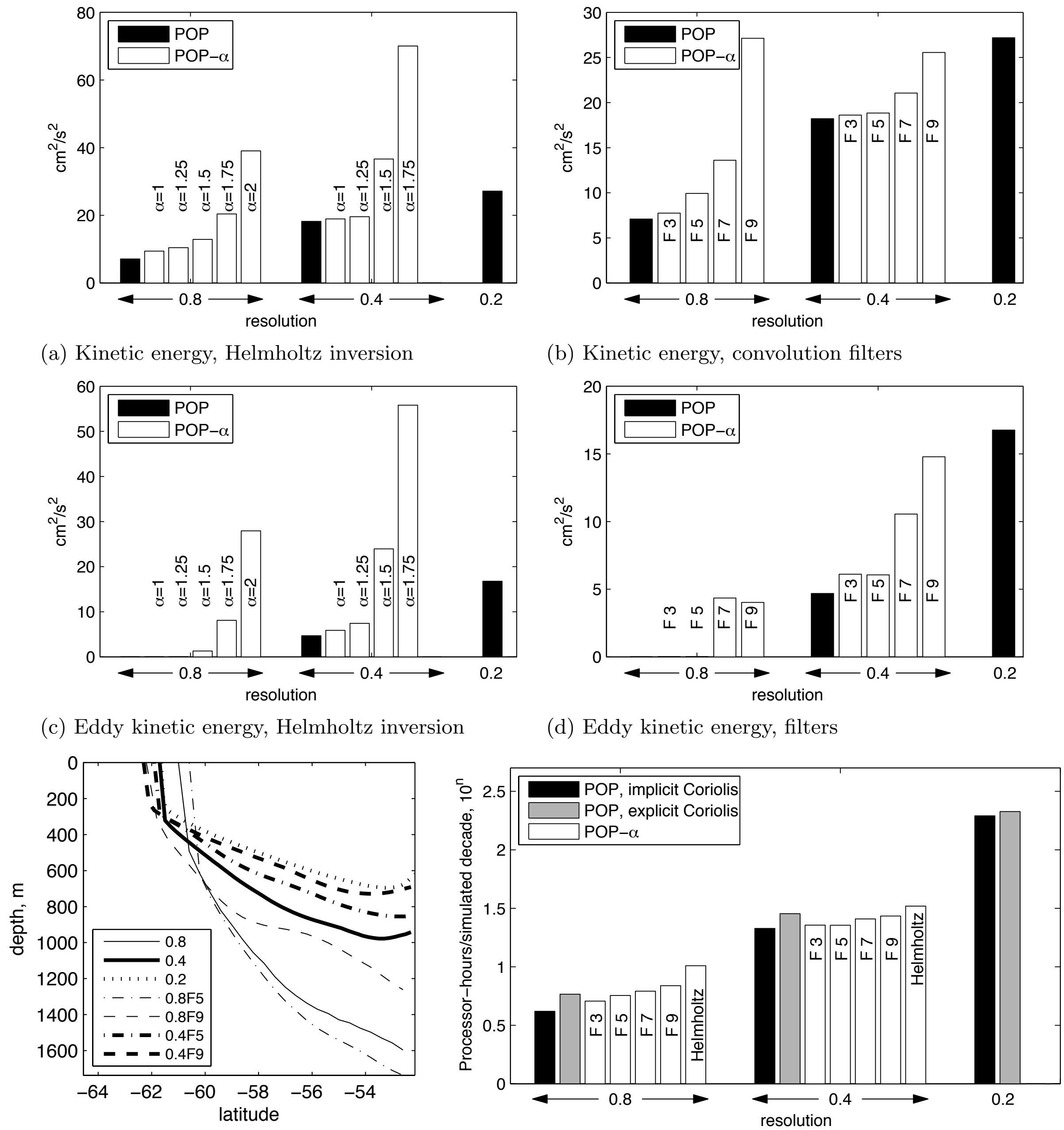

(a) Kinetic energy, Helmholtz inversion

(b) Kinetic energy, convolution filters

(c) Eddy kinetic energy, Helmholtz inversion

(d) Eddy kinetic energy, filters

(e) 6^oC isotherm depth, filters

(f) computation time

Figure 2. Comparison of turbulence statistics produced by POP, POP-α with smoothing by the Helmholtz inversion, and POP-α with smoothing by convolution filters. Identifiers such as 0.8 refer to an $0.8^o \times 0.8^o$ grid. The α parameter controls the strength of smoothing by the Helmholtz inversion, while the stencil width (F3–F9) controls smoothing strength for the filters. In general, the LANS-α model improves all turbulence statistics with only minor addition of computational cost in the more efficient implementations. These figures reprinted from *Petersen et al.* [2008].

Our method of scaling biharmonic and Laplacian viscous coefficients can be readily extended to the scaling and joint application of biharmonic and Laplacian diffusive coefficients, with the caveat that biharmonic forms of GM90 are difficult to implement in z-coordinate models.

We have touched in brief on the issue of adiabatic tracer mixing, as it remains of concern even at eddy-resolving scale. Issues of mixing cannot be entirely isolated from the choice of transport scheme, and this topic also has been touched on briefly in our effort to survey a number of issues associated with the choice of lateral mixing parameterizations for eddy-resolving ocean modeling.

The LANS-α model offers an entirely different approach to subgridscale turbulence parameterization and should be seen as a more sophisticated option for use in conjunction with conventional viscous and diffusive parameterizations to bring out more realistic levels of variability at what would otherwise be eddy-admitting resolutions. It is important here to understand that effective use of the POP-α model does not parameterize the effect of eddies, but more readily allows for the inclusion of eddies. Eddy flux parameterizations based on *Gent and McWilliams* [1990] have been a tremendous boon to ocean and climate modeling, and yet they do not capture all of the important effects of eddies, as discussed, for instance, in *Eden et al.* [2007], where eddy tracer fluxes are identified as being upgradient over much of the Gulf Stream region.

An open question in eddy-resolving ocean modeling, partially addressed in BHS07, is the question of how much of the benefit of grid refinement is associated with increased levels of mesoscale eddy variability, and how much may be attributable simply to better resolution of the topography. Unquestionably, the former is of considerable importance, and to the extent this is true the LANS-α model offers a possible means to obtain more realistic feedback of the eddy variability on the mean at around half the resolution as required for a conventional eddy-resolving ocean model. The order-of-magnitude savings in computational cost associated with this step back in resolution makes this method attractive for use in climate science.

Acknowledgments. We wish to acknowledge Robert Hallberg for a conversation that eventually led to our reconsideration of the joint use of biharmonic and Laplacian viscosity, Stephen Griffies for insightful comments as a reader, and two anonymous reviewers for their essential contributions. This work was supported by the Department of Energy's Office of Science. Los Alamos National Laboratory is operated by Los Alamos National Security, LLC for the Department of Energy.

References

Adcroft, A., C. Hill, and J. Marshall, Representation of topography by shaved cells in a height coordinate ocean model, *Mon. Weather Rev.*, *125*, 2293–2315, 1997.

Adcroft, A., J. Campin, P. Heimbach, C. Hill, and J. Marshall, MIT-gcm manual, *Tech. rep.*, MIT, http://mitgcm.org/pelican/online_documents/manual.html, 2005.

Andrews, D. B., and M. E. McIntyre, An exact theory of nonlinear waves on a Lagrangian-mean flow, *J. Fluid Mech.*, *89*, 609–646, 1978.

Bleck, R., An oceanic general circulation model framed in hybrid isopycnic-cartesian coordinates, *Ocean Modelling*, *37*, 55–88, 2002.

Bryan, F. O., M. W. Hecht, and R. D. Smith, Resolution convergence and sensitivity studies with North Atlantic circulation models. Part I: The western boundary current system, *Ocean Modelling*, *16*(3–4), 141–159, doi: 10.1016/j.ocemod.2006.08.005, 2007.

Chassignet, E. P., and Z. D. Garraffo, Viscosity parameterization and Gulf Stream separation, in *Proceedings of the 'Aha Huliko'a Hawaiian Winter Workshop*, edited by P. Muller and D. Henderson, pp. 367–374, U. Hawaii, 2001.

Chen, S., C. Foias, D. D. Holm, E. Olson, E. S. Titi, and S. Wynne, Camassa-Holm Equations as a Closure Model for Turbulent Channel and Pipe Flow, *Phys. Rev. Lett.*, *81*, 5338–5341, doi:10.1103/PhysRevLett.81.5338, 1998.

Chen, S., C. Foias, D. D. Holm, E. Olson, E. S. Titi, and S. Wynne, The Camassa-Holm equations and turbulence, *Physica D: Nonlinear Phenomena*, *133*, 49–65, 1999a.

Chen, S., D. D. Holm, L. G. Margolin, and R. Zhang, Direct numerical simulations of the Navier-Stokes alpha model, *Physica D: Nonlinear Phenomena*, *133*, 66–83, 1999b.

Delhez, E. J. M., and E. Deleersnijder, Overshootings and spurious oscillations caused by biharmonic mixing, *Ocean Modelling, in press*, doi:10.1016/j.ocemod.2007.01.002, 2007.

Domaradzki, J. A., and D. D. Holm, Navier-Stokes-alpha model: LES equations with nonlinear dispersion, *Special LES volume of ERCOFTAC Bulletin*, *48*, 2001.

Eden, C., R. J. Greatbatch, and J. Willebrand, A diagnosis of thickness fluxes in an eddy-resolving model, *J. Phys. Oceanogr.*, *37*(3), 727–742, doi:10.1175/JPO2987.1, 2007.

Foias, C., D. D. Holm, and E. S. Titi, The Navier-Stokes-alpha model of fluid turbulence, *Physica D: Nonlinear Phenomena*, *152-153*, 505 – 19, 2001a.

Foias, C., D. D. Holm, and E. S. Titi, The Navier-Stokes-alpha model of fluid turbulence, *Physica D: Nonlinear Phenomena*, 2001b.

Gent, P. R., and J. C. McWilliams, Isopycnal mixing in ocean circulation models, *J. Phys. Oceanogr.*, *20*, 150—155, 1990.

Geurts, B. J., and D. D. Holm, Regularization modeling for large-eddy simulation, *Phys. Fluids*, *15*(L13-L16), 2003.

Griffies, S., R. Pacanowski, and R. Hallberg, Spurious diapycnal mixing associated with advection in a z-coordinate ocean model, *Mon. Weather Rev.*, *128*, 538–564, 2000.

Griffies, S. M., *Fundamentals of Ocean Climate Models*, Princeton University Press, 2004.

Griffies, S. M., and R. W. Hallberg, Biharmonic friction with a Smagorinsky-like viscosity for use in large-scale eddy-permitting ocean models, *Mon. Weather Rev.*, *128*, 2935–2946, 2000.

Hallberg, R., and A. Gnanadesikan, The role of eddies in determining the structure and response of the wind-driven Southern Hemisphere overturning: Results from the Modeling Eddies in the Southern Ocean (MESO) Project, *J. Phys. Oceanogr.*, *36*, 2232–2252, 2006.

Hecht, M. W., and R. D. Smith, Towards a physical understanding of the North Atlantic: A review of model studies in an eddying regime, in *Ocean Modeling in an Eddying Regime*, edited by M. Hecht and H. Hasumi, Geophysical Monograph Series, American Geophysical Union, 2008.

Hecht, M. W., W. R. Holland, and P. J. Rasch, Upwind-weighted advection schemes for ocean tracer transport: An evaluation in a passive tracer context, *J. Geophys. Res.*, *100*, 20,763—20,778, 1995.

Hecht, M. W., F. O. Bryan, M. Maltrud, and R. D. Smith, The Northwest Corner of the Atlantic and rapid climate change, Los Alamos National Laboratory report, LA-UR-06-7346; available at http://www.noc.soton.ac.uk/rapid/rapid2006/ic06pres.php, 2006.

Hecht, M. W., D. D. Holm, M. R. Petersen, and B. A. Wingate, Implementation of the LANS-alpha turbulence model in a primitive equation ocean model, *J. Comput. Phys.*, doi: 10.1016/j.jcp.2008.02.018, 2008.

Holland, W. R., F. O. Bryan, and J. C. Chow, Application of a third-order upwind scheme in the NCAR Ocean Model, *J. Clim.*, *11*, 1487—1493, 1998.

Holm, D., C. Jeffery, S. K. Kurien, D. Livescu, M. Taylor, and B. Wingate, The LANS-α model for computing turbulence: Origins, results, and open problems, *LA Science*, *29*, 152, 2005.

Holm, D. D., Fluctuation effects on 3d lagrangian mean and eulerian mean fluid motion, *Physica D: Nonlinear Phenomena*, *133*, 215–269, 1999.

Holm, D. D., Averaged Lagrangians and the mean effects of fluctuations in idea fluid dynamics, *Physica D: Nonlinear Phenomena*, *2875*, 1–34, 2002.

Holm, D. D., and B. T. Nadiga, Modeling mesoscale turbulence in the barotropic double-gyre circulation, *J. Phys. Oceanogr.*, *33*, 2355–2365, 2003.

Holm, D. D., and B. A. Wingate, Baroclinic instabilities of the two-layer quasigeostrophic alpha model, *J. Phys. Ocgr. in review*, pp. 1287–1296, 2005.

Holm, D. D., J. E. Marsden, and T. S. Ratiu, Euler-Poicaré models of ideal fluids with nonlinear dispersion, *Phys. Rev. Lett*, *80*, 4173–4177, 1998.

Hundsdorfer, W., and R. A. Trompert, Method of lines and direct discretization: a comparison for linear advection, *Applied numerical mathematics*, *13*(6), 469 – 90, 1994.

Hunke, E., M. Maltrud, and M. Hecht, On the grid dependence of lateral mixing parameterizations for global ocean simulations, *Ocean Modelling*, *20*, 115–133, doi: 10.1016/j.ocemod.2007.06.010, 2008.

Hurlburt, H. E., and P. J. Hogan, Impact of 1/8° to 1/64° resolution on Gulf Stream model–data comparisons in basin-scale subtropical Atlantic Ocean models, *Dyn. Atmos. Ocean*, *32*(3-4), 283–329, 2000.

Lee, M.-M., A. C. Coward, and A. J. G. Nurser, Spurious diapycnal mixing of the deep waters in an eddy-permitting global ocean model, *J. Phys. Oceanogr.*, *32*(5), 1522 – 35, 2002.

Lindsay, K., A class of flux limited advection schemes applied to ocean models, *Ocean Modelling*, submitted, 2007.

Maltrud, M. E., and J. L. McClean, An eddy resolving 1/10° ocean simulation, *Ocean Modelling*, *8*(1–2), 31–54, 2005.

Munk, W. H., On the wind-driven ocean circulation, *J. Meteorol.*, *7*(2), 79 – 93, 1950.

Özgökmen, T. M., E. P. Chassignet, and A. M. Paiva, Impact of wind forcing, bottom topography, and inertia on midlatitude jet separation in a quasigeostrophic model, *J. Phys. Oceanogr.*, *27*, 2460–2476, 1997.

Petersen, M. R., M. W. Hecht, and B. A. Wingate, Efficient form of the LANS-alpha turbulence model in a primitive-equation ocean model, *J. Comput. Phys.*, doi:10.1016/j.jcp.2008.02.017, 2008.

Roberts, M., and D. Marshall, Do we require adiabatic dissipation schemes in eddy-resolving ocean models?, *J. Phys. Oceanogr.*, *28*(10), 2050 – 63, 1998.

Rossby, T., The North Atlantic Current and surrounding waters: At the crossroads, *Rev. Geophys.*, *34*(4), 463–481, 1996.

Semtner, A. J., and Y. Mintz, Numerical simulation of the Gulf Stream and mid-ocean eddies, *J. Phys. Oceanogr.*, *7*(2), 208 – 30, 1977.

Smith, R. D., and P. Gent, Reference manual of the Parallel Ocean Program (POP), *Los Alamos National Laboratory report LA-UR-02-2484*, Los Alamos National Laboratory, Los Alamos, NM, 2002.

Smith, R. D., and P. R. Gent, Anisotropic GM parameterization for ocean models, *J. Phys. Oceanogr.*, *34*, 2541–2564, doi: 10.1175/JPO2613.1, 2004.

Smith, R. D., and J. C. McWilliams, Anisotropic horizontal viscosity for ocean models, *Ocean Modelling*, *5*, 129–156, 2003.

Smith, R. D., M. E. Maltrud, F. O. Bryan, and M. W. Hecht, Numerical simulation of the North Atlantic Ocean at $\frac{1}{10}^\circ$, *J. Phys. Oceanogr.*, *30*, 1532–1561, 2000.

Veronis, G., *Numerical Models of Ocean Circulation*, chap. The role of models in tracer studies, pp. 133–146, Natl. Acad. Sci., 1975.

Weese, S. R., and F. O. Bryan, Climate impacts of systematic errors in the simulation of the path of the North Atlantic Current, *Geophys. Res. Lett.*, *33*(19), L19,708 –, doi: 10.1029/2006GL027669, 2006.

Wingate, B. A., The maximum allowable time step for the shallow water α model and its relation to time-implicit differencing, *Mon. Weather Rev.*, *132*, 2719–2731, 2004.

M. W. Hecht, Computational Physics Group, CCS Division, Mail Stop B296, Los Alamos National Laboratory, Los Alamos, NM, 87545, USA. (mhecht@lanl.gov)

E. C. Hunke, Fluid Dynamics Group, Theoretical Division, Mail Stop B216, Los Alamos National Laboratory, Los Alamos, NM, 87545, USA. (eclare@lanl.gov)

M. E. Maltrud, Fluid Dynamics Group, Theoretical Division, Mail Stop B216, Los Alamos National Laboratory, Los Alamos, NM, 87545, USA. (maltrud@lanl.gov)

M. R. Petersen, Computational Physics Group, CCS Division, Mail Stop B296, Los Alamos National Laboratory, Los Alamos, NM, 87545, USA. (mpetersen@lanl.gov)

B. A. Wingate, Computational Physics Group, CCS Division, Mail Stop D413, Los Alamos National Laboratory, Los Alamos, NM, 87545, USA. (wingate@lanl.gov)